A Time-Resolved FTIR Difference Study of the Plastoquinone Q_A and Redox-Active Tyrosine Y_Z Interactions in Photosystem II

Haoming Zhang,*,‡ M. Reza Razeghifard,§ Gad Fischer,§ and Tom Wydrzynski*,‡

Research School of Biological Sciences, Institute of Advanced Studies, and Department of Chemistry, Faculty of Science, The Australian National University, Canberra, Australia 0200

Received April 8, 1997; Revised Manuscript Received June 19, 1997⊗

ABSTRACT: In this paper, we present the first time-dependent measurements of flash-induced infrared difference spectra of photosystem II (PSII) using Fourier transform infrared (FTIR) spectroscopy. With this experimental approach, we were able to obtain the $Y_Z^{ox}Q_A^-/Y_ZQ_A$ vibrational difference spectrum of Tris-washed, PSII-enriched samples in the absence of hydroxylamine at room temperature (16 ± 2 °C), with a spectral resolution of 4 cm^{-1} and a temporal resolution of 50 ms. In order to determine the dominant species in the FTIR spectrum at a particular point in time after an excitation flash, the decay kinetics of Y_Z^{ox} and Q_A^- were independently monitored by EPR and chlorophyll *a* fluorescence, respectively, under the same experimental conditions. These measurements confirmed that the addition of DCMU to Tris-washed PSII samples does not significantly affect the Y_Z^{ox} decay, but does substantially slow down the Q_A^- decay. By making use of the difference in the decay kinetics using DCMU, the Q_A^-/Q_A signals could be separated from the Y_Z^{ox}/Y_Z signals and a pure Q_A^-/Q_A difference spectrum obtained. By comparison of the $Y_Z^{ox}Q_A^-/Y_ZQ_A$ difference spectrum with the pure Q_A^-/Q_A difference spectrum, a large differential band at 1706/1699 cm^{-1} could be identified and associated with Y_Z oxidation. In contrast, an intense band at 1478 cm^{-1}, whose DCMU-sensitive decay follows the Q_A^- decay based on the chlorophyll *a* fluorescence measurements, was present in all of the time-resolved spectra. Since no significant reversible Chl^+ radicals could be detected by the EPR measurements under our experimental conditions, we confirm that this band most likely arises only from the semiquinone anion Q_A^- [Berthomieu, C., Nabedryk, E., Mäntele, W., & Breton, J. (1990) *FEBS Lett. 269*, 363−367].

Photosynthetic water oxidation occurs in photosystem II (PSII)[1] of plants, algae and cyanobacteria. Among its over 25 protein subunits, the D1 and D2 proteins of PSII form the reaction center (RC) and are believed to bind most of the prosthetic groups involved in electron transport leading to water oxidation [for a review, see Debus (1992)]. In PSII, the primary charge separation event is initiated by the absorption of a photon by P_{680}, the photoactive chlorophyll *a* molecule located in the RC. The excited P_{680}* transfers one electron to a bound pheophytin molecule, forming the $P_{680}^+Phe^-$ radical pair in a few picoseconds (Schelvis et al., 1994). The charge separation is further stabilized by the subsequent rapid electron transfer to the primary acceptor plastoquinone Q_A and then to the secondary acceptor plastoquinone Q_B. Oxidized P_{680}^+ is reduced by a redox-active tyrosine residue Y_Z and Y_Z^{ox} in turn oxidizes a cluster of four Mn ions which catalyze water oxidation through the cycling of five intermediate states (S_i where $i = 0-4$).

In addition to Y_Z, PSII has another redox-active tyrosine residue, Y_D. Both oxidized tyrosine residues give rise to EPR signals with very similar line shapes [for reviews, see Barry (1993) and Hoganson and Babcock (1994)]. It is believed that both Y_Z^{ox} and Y_D^{ox} are neutral radicals with the phenolic oxygen deprotonated (Barry & Babcock, 1987). EPR studies of site-directed mutants in the cyanobacterial *Synechocystis* PCC 6803 have revealed that Y_Z is Tyr-161 of the D1 protein and Y_D is Tyr-160 of the D2 protein (Debus et al., 1988; Metz et al., 1989; Vermaas et al., 1988). Despite similar EPR signals, Y_Z^{ox} and Y_D^{ox} have dramatically different functions and decay kinetics. It is known that Y_D is not directly involved in electron transport leading to water oxidation since Y_D-deletion mutants still can grow photoautotrophically (Debus et al., 1988; Vermaas et al., 1988). In intact PSII, Y_D^{ox} is dark-stable for hours, while the decay of Y_Z^{ox} occurs in the microsecond range and is S_i-state-dependent (Babcock & Sauer, 1975b; Dekker et al., 1984). Removal of the Mn cluster slows down the Y_Z^{ox} decay to the millisecond regime and exposes Y_Z^{ox} to exogenous reductants such as ferrocyanide (Babcock & Sauer, 1975a; Ghanotakis et al., 1982; Yerkes & Babcock, 1980). Removal of Mn also results in the direct oxidation of Y_D by P_{680}^+ (Debus et al., 1988).

On the acceptor side of PSII, Q_A acts as a one-electron acceptor, while Q_B acts as a two-electron gate. Upon receiving two electrons, Q_B is protonated as Q_BH_2 and replaced by another plastoquinone molecule from the PQ pool. A non-heme Fe^{2+} interacts between Q_A and Q_B. In

* To whom correspondence should be addressed.
‡ Research School of Biological Sciences, Institute of Advanced Studies.
§ Department of Chemistry, Faculty of Science.
⊗ Abstract published in *Advance ACS Abstracts,* August 15, 1997.
[1] Abbreviations: Chl, chlorophyll; DCMU, 3-(3,4-dichlorophenyl)-1, 1-dimethylurea; DMSO, dimethyl sulfoxide; EPR, electron paramagnetic resonance; TR-FTIR, time-resolved Fourier transform infrared; Mes, 2-(*N*-morpholino)ethanesulfonic acid; P_{680}, primary electron donor of PSII; PSII, photosystem II; Q_A, primary plastoquinone acceptor; Q_B, secondary plastoquinone acceptor; RC, reaction center; Tris, tris-(hydroxymethyl)aminomethane; Y_D, tyrosine D; Y_Z, tyrosine Z.

S0006-2960(97)00815-5 CCC: $14.00

the absence of DCMU, the non-heme Fe^{2+} in PSII can be oxidized by ferricyanide, and the oxidized non-heme Fe^{3+} is reduced by Q_A^- on a microsecond time scale (Bowes et al., 1979; Ikegami & Katoh, 1973). The risetime for the oxidation of the non-heme Fe^{2+} is much longer with a half-time of ~20 s in Tris-washed PSII at pH 8 (Hienerwadel & Berthomieu, 1995).

FTIR difference studies have been carried out to investigate vibrational properties upon the photoreduction of Q_A and photooxidation of Y_Z. The light-induced FTIR difference spectrum of Q_A^-/Q_A in PSII was first characterized by Berthomieu et al. (1990). The spectrum was obtained after 1 s continuous illumination of PSII samples in the presence of NH_2OH and DCMU. The rapid reduction of Y_Z^{ox} by NH_2-OH and the blockage of electron flow from Q_A^- to Q_B by DCMU allow Q_A^- to be stable for hours, which enables sufficient time for signal averaging. On the basis of FTIR measurements of quinone redox reactions *in vitro* (Bauscher et al., 1990), an intense band at 1478 cm^{-1} in the Q_A^-/Q_A difference spectrum was tentatively assigned to the υ(CO) mode of the semiquinone anion Q_A^- (Berthomieu et al., 1990). In support of this assignment, this band was found to be insensitive to ^{15}N-labeling of spinach PSII (Berthomieu et al., 1992). The assignment of the 1478 cm^{-1} band solely to the υ(CO) mode of Q_A^- was, however, questioned by MacDonald et al. (1995) since a slowly-decaying Chl^+ radical was observed in ~5% of the PSII RCs in the presence of NH_2OH under continuous illumination at −9 °C. Moreover, the 1478 cm^{-1} band was downshifted by 2 cm^{-1} in global ^{15}N-labeled PSII samples from *Synechocystis* sp. PCC 6803. Thus, it was argued that the 1478 cm^{-1} band contains contributions from Chl^+ radicals as well. Recently, Hienerwadel et al. (1996) reinvestigated the Q_A^-/Q_A spectrum using flash excitation and confirmed under their conditions that the 1478 cm^{-1} band arises only from Q_A^-. Likewise, the 1478 cm^{-1} band was also observed in the $S_2Q_A^-/S_1Q_A$ difference spectrum obtained at low temperature (250 K) in the absence of NH_2OH (Noguchi et al., 1992). In addition, discrepencies also exist as to the infrared Y_Z signals. It has been suggested that the υ(C−O) mode of Y_Z^{ox} contributes at 1477 cm^{-1} (Bernard et al., 1995; MacDonald et al., 1993), while it was argued that this band may be contaminated by the Q_A^- signal (Hienerwadel et al., 1996). Thus, the band assignments with regard to both Q_A and Y_Z remain incomplete, in spite of a number of investigations.

So far, almost all FTIR difference studies on light-induced reactions in PSII have focused on static measurements where experimental conditions are used to photoaccumulate one dominating species. As to the infrared decay kinetics of Q_A and Y_Z, little information is available. In an earlier work, Hienerwadel et al. (1992) studied the decay kinetics of Q_A^- by a monochromatic IR technique, where the decay of only one spectral band was obtained. In contrast, however, TR-FTIR spectroscopy is a broad-band technique and has the advantage of obtaining the time-dependence across a wide spectral range, which can be used to kinetically discriminate redox intermediates. For example, Thibodeau et al. (1990) used TR-FTIR spectroscopy to study the decay kinetics of redox intermediates in the bacterial RCs from *Rb. sphaeroides* following a short continuous illumination. In this paper, we use TR-FTIR spectroscopy for the first time to investigate the single flash-induced $Y_Z^{ox}Q_A^-/Y_ZQ_A$ difference spectrum in Tris-washed, PSII-enriched samples at room temperature in the absence of hydroxylamine.

MATERIALS AND METHODS

Sample Preparations. PSII-enriched membranes were prepared from hydroponically grown spinach with Triton X-100 treatment as described earlier (Berthold et al., 1981). The steady-state oxygen-evolving activity of the prepared PSII-enriched membranes was 500−610 μmol (mg of Chl)$^{-1}$ h^{-1} in the presence of 1 mM ferricyanide and 50 μM PPBQ at 25 °C. The oxygen-evolving capacity was destroyed by treatment with Tris at 0.5 M (pH 8.0) concentration in room light for 15 min at 4 °C. The treated PSII samples were then washed and resuspended in a buffer medium containing 40 mM Mes and 10 mM NaCl (pH 6.0). 10 mM potassium ferri/ferrocyanide (ratio 1/1) was added to the sample suspension followed by ultracentrifugation at 100000*g* for 15 min to form a solid pellet. In the case where electron flow from Q_A to Q_B is blocked, 0.1 mM DCMU dissolved in DMSO was added to the sample suspension after Tris washing (final concentration of DMSO is ~1%) and incubated for 10 min in the dark followed by ultracentrifugation in the presence of 10 mM ferri/ferocyanide.

FTIR Measurements. Transient infrared spectra of PSII samples after photoexcitation were recorded on a Bruker IFS 66 spectrometer equipped with a liquid nitrogen-cooled MCT-B detector and a KBr beam splitter. The FTIR spectrometer was set up in a rapid scan mode. Under the optimal S/N condition, a scanner velocity of 2.53 cm/s was used, which yielded a time resolution of 50 ms per interferogram at 4 cm^{-1} resolution. The spectra were reproducible to ±1 cm^{-1}. After a single saturating flash, a train of seven infrared transient spectra were recorded on the single side of the interferogram. The dark spectrum was measured 120 ms before the photoexcitation and used as a background spectrum to construct the final difference spectrum. Since the time interval between the dark and light spectra was short, variations arising from the light source and slowly-changing environmental factors were largely suppressed. To further improve the S/N, the process was cycled with a flash frequency of 0.2 or 1 Hz, as designated in the text. The final spectrum was averaged over 4000 scans. The entire measurement took ~1.1 h at 1 Hz flash frequency and ~5.5 h at 0.2 Hz flash frequency. The timing for each trace and for synchronization between data acquisition and photoexcitation was controlled by an internal clock with an accuracy of 1 μs. A typical timing sequence for one cycle is shown in Figure 1.

Photoexcitation of the PSII samples was provided by a 5 μs (FWHH) xenon flash lamp which was triggered by a TTL pulse from the FTIR spectrometer. An optical fiber was used as a light guide for excitation of the PSII samples directly in the sample chamber. Infrared radiation from the xenon flash lamp was filtered out using a short-pass infrared filter (OCLI). Three saturating preflashes, spaced 1 s or 5 s, were given to the PSII samples prior to data acquisition in order to reduce the non-heme Fe^{3+} and to oxidize Y_D that may have formed during the dark period of sample handling.

A part of the PSII pellet sample was deposited and sealed between two CaF_2 windows. The absorbance at the amide I band (1657 cm^{-1}) was adjusted to be ~0.75 AU. A Ge filter (OCLI) was placed in front of the sample chamber to

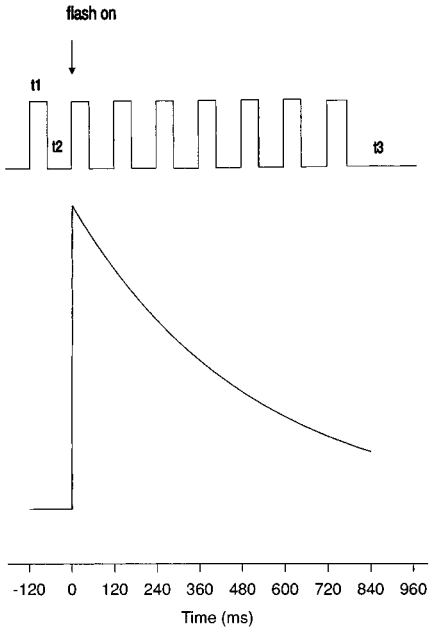

FIGURE 1: Schematic diagram of TR-FTIR timing for one measuring cycle where t1, t2, and t3 represent the time resolution, the time interval between two consecutive traces, and the waiting period (1 or 5 s) for closed reaction centers to recover, respectively.

block out the red He−Ne laser beam. All measurements were performed at room temperature (16 ± 2 °C).

EPR Measurements. Room temperature EPR measurements were performed at X-band on a Bruker ESP 300E spectrometer equipped with a TM101 cavity. A part of the same PSII sample used for the FTIR measurement was deposited on a tissue cell to obtain the EPR spectrum. For kinetic measurements of signal II_f (EPR Y_Z^{ox} signal in Tris-washed PSII), a xenon flash lamp (5 μs, FWHH) was used to excite the PSII sample in the cavity, while a slide projector was used as a continuous light source to obtain the EPR signals. The Y_Z^{ox} kinetics were measured from the downfield peak of signal II_s (EPR Y_D^{ox} signal) as described by Razeghifard et al. (1997).

Chlorophyll a Fluorescence Measurements. Flash-induced chlorophyll *a* fluorescence decay kinetics of PSII samples were measured at room temperature on a PAM 101 pulse-modulated fluorometer. A part of the same PSII sample used for the FTIR and EPR measurements was deposited on a glass plate and placed in the sample chamber. Weak monitoring flashes ($\lambda = 650$ nm, 1 μs duration) were applied at 1.6 kHz. The saturating actinic flash (3.5 μs, FWHH) was provided by a xenon flash lamp filtered through a Schott BG-18 filter. The photodiode detector was protected by a RG-715 filter. Data acquisition and flash-triggering were controlled by a PC computer using a DA-100 data acquisition system. Three actinic preflashes were given in the sample chamber prior to data acquisition.

RESULTS AND DISCUSSION

Characterization of Y_Z^{ox} and Q_A^- Decay Kinetics. Chlorophyll *a* fluorescence measurements provide a convenient, noninvasive method for monitoring the population of Q_A^-. In the dark, the level of the chlorophyll *a* fluorescence is low due to the quenching effect of Q_A. After photoexcitation, the chlorophyll *a* fluorescence rises to a maximal level as the $Y_Z^{ox}P_{680}Q_A^-$ state is formed. Reoxidation of Q_A^- via

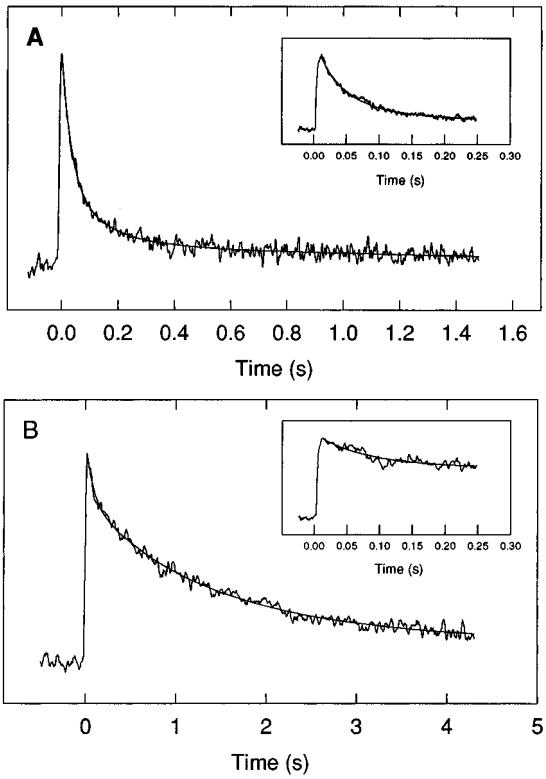

FIGURE 2: Flash-induced chlorophyll *a* fluorescence decay kinetics of Tris-washed PSII samples in the presence of 10 mM ferri/ferrocyanide at pH 6.0. (A) Minus DCMU; (B) plus 0.1 mM DCMU. All measurements were performed at room temperature, and three preflashes were given to the PSII samples prior to data acquisition. Insets: the signals were measured in a shorter time region with instrumental time constants of 17 μs. Each spectrum is an average of three traces.

various electron pathways in PSII will then lead to the decay of the chlorophyll *a* fluorescence intensity.

Figure 2 shows the single flash-induced chlorophyll *a* fluorescence decay kinetics of Tris-washed PSII samples in the presence of 10 mM ferri/ferrocyanide at pH 6.0. In the absence of DCMU (Figure 2A), about 94% of the signal decays within 1 s after the flash. By contrast, in the presence of DCMU (Figure 2B), the fluorescence decay is significantly slower. In this situation, approximately 55% of the signal decays within 1 s after the flash. According to the fluorescence decay recorded on a longer time scale (data not shown), about 91% of the PSII RCs decay within 5 s after the flash excitation.

EPR was used as an independent method to monitor the decay kinetics of signal II in the same PSII samples used for the FTIR measurements. Figure 3 shows the spectra of the signal II region of Tris-washed PSII samples under continuous illumination. In the absence of DCMU (Figure 3A), continuous illumination of PSII samples generates both Y_Z^{ox} and Y_D^{ox}. The amplitude of signal II in the light (trace a) is about 1.5 times larger than that measured 10 s after illumination (trace b), which indicates the generation of the Y_Z^{ox} radical under continuous illumination. The fast decrease in the signal amplitude following illumination represents the rapid decay of Y_Z^{ox} in the dark. The subsequent slow decrease in the signal amplitude (traces c and d) is due to the decay of Y_D^{ox}, which has a half-time of a few tens of minutes. In the presence of DCMU (Figure 3B), the Y_Z^{ox} signal is almost inhibited due to the photoaccumulation of inactive state $Y_ZP_{680}Q_A^-$ under continuous illumination

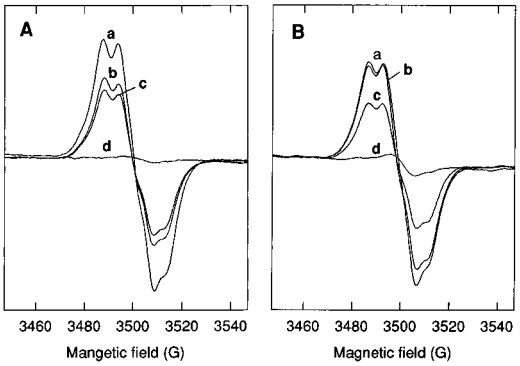

FIGURE 3: Room temperature EPR signal II spectra under continuous illumination in Tris-washed PSII samples in the presence of 10 mM ferri/ferrocyanide at pH 6.0. (A) Minus DCMU; (B) plus 0.1 mM DCMU. Traces: a, in light; b, 10 s after light; c, 5 min after light; d, 60 min after light. Experimental conditions: microwave power, 4 mW; modulation amplitude, 4 G; modulation frequency, 100 kHz; microwave frequency, 9.8 GHz.

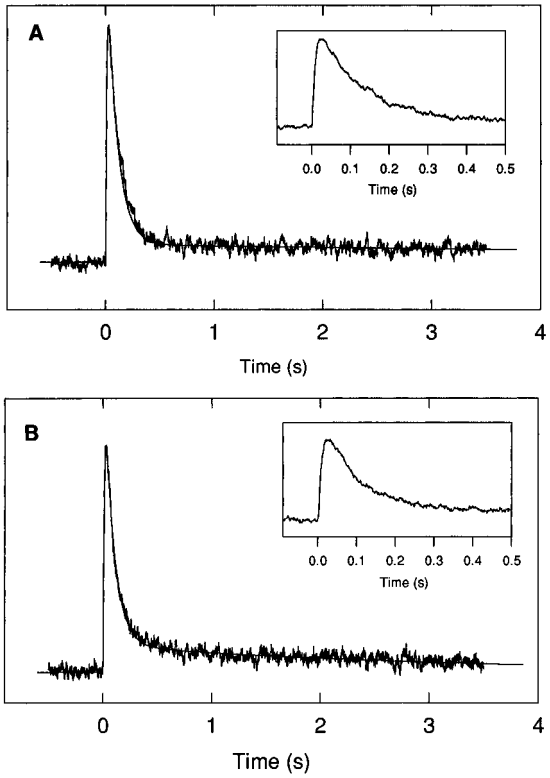

FIGURE 4: Room temperature EPR signal II decay kinetics of Tris-washed PSII samples in the presence of 10 mM ferro/ferricyanide at pH 6.0. (A) Minus DCMU; (B) plus 0.1 mM DCMU. Experimental conditions: microwave power, 100 mW; modulation amplitude, 4 G; modulation frequency, 100 kHz; microwave frequency, 9.8 GHz; time constant, 10 ms. Averaged over 50 traces with 5 s between flashes. Insets: the decay kinetics are shown on expanded time scales.

(Ghanotakis et al., 1983). The observed signal in the light (trace a) mainly arises from Y_D^{ox}. Under this condition, the decay of Y_D^{ox} is also slow. In both cases, no signals due to reversible Chl^+ radical formation are obvious. A dark-stable radical is, however, observed after long dark-adaptation (~60 min). This radical does not contribute to the FTIR difference spectra which are recorded during a fast photocycle (0.2 or 1 Hz).

Figure 4 shows the signal II decay kinetics measured on the downfield side of signal II_s. In contrast to continuous illumination, under the flash excitation, the Y_Z^{ox} decay is observable in the presence of DCMU (Figure 4B) due to the reoxidation of Q_A^- between flashes. In the presence and absence of DCMU, the signal II decay is biphasic. The fast and slow components represent the decay of Y_Z^{ox} and Y_D^{ox}, respectively. Analysis of the fast decay kinetics gives half-times of 110 and 95 ms in the absence and presence of DCMU, respectively, indicating that DCMU has relatively little effect on the Y_Z^{ox} decay.

In Tris-washed PSII samples, the reduction of Y_Z^{ox} and the reoxidation of Q_A^- basically involve two processes: (1) charge recombination between Y_Z^{ox} and Q_A^- in a fraction of PSII RCs and (2) redox reactions with exogenous electron acceptor and donors in the rest of PSII RCs. With DCMU present, reoxidation of Q_A^- by ferricyanide is slower than without DCMU present as revealed by the variable chlorophyll *a* fluorescence measurement (Figure 2). This difference may arise from the fact that the Q_B site is more accessible to the exogenous oxidants than the Q_A site. It is known that the Q_B site is situated in a more polar and surface-exposed environment than the Q_A site (Ruffle et al., 1992), which may allow more efficient electron flow to ferricyanide. The slow reoxidation of Q_A^- by ferricyanide in the presence of DCMU could result in a fraction of PSII RCs closed under high flash frequency. Thus, to ensure most of the PSII RCs turn over during FTIR measurements, we used 0.2 Hz flash frequency for DCMU-treated PSII samples. When DCMU is absent, there is a tradeoff between flash frequency and prevention of the non-heme iron oxidation by ferricyanide. In this case, a 1 Hz flash frequency was used since ~94% of the PSII RCs are open (Figure 2A) and the oxidation of the non-heme iron is negligible within 1 s after photoexcitation (see below).

Analysis of TR-FTIR Difference Spectra. The FTIR kinetic difference spectra arising from the $Y_Z^{ox}Q_A^-/Y_ZQ_A$ state are shown in Figure 5. The spectra were measured in the presence of 10 mM ferri/ferrocyanide and 0.1 mM DCMU with 0.2 Hz flash frequency. Under these conditions, neither will Y_D contribute to the difference spectra because of its slow turnover nor will P_{680} and Phe contribute because of their fast decay on the microsecond scale. The flash-induced difference spectrum should thus contain only contributions from Y_Z and Q_A and/or any other protein side chains and protein backbones perturbed by the photochemical reactions of Y_Z and Q_A. The positive and negative bands in the spectra correspond to the absorptions related to the $Y_Z^{ox}Q_A^-$ and Y_ZQ_A states, respectively. Ferri/ferrocyanide has no contributions in the spectral region between 1800 and 1200 cm^{-1}.

As shown in Figure 5 (inset), the characteristic υ(CN) ferri/ferrocyanide absorptions at 2116 and 2040 cm^{-1} are observed after excitation, indicating that electron transport indeed occurs in the PSII sample during the FTIR measurements. The net level of ferri- and ferrocyanide is determined by the rate of Y_Z^{ox} reduction by ferrocyanide and the rate of Q_A^- oxidation by ferricyanide. The positive band at 2116 cm^{-1} and the negative band at 2040 cm^{-1} indicate that the rate of Y_Z^{ox} reduction is faster than the rate of Q_A^- oxidation, which is consistent with the fluorescence and EPR measurements under these conditions (Figures 2 and 4). For the time domain used for recording trace a, there should be more than 80% Y_Z^{ox} and Q_A^- present (Figures 2 and 4). Thus, trace a is attributed to the $Y_Z^{ox}Q_A^-/Y_ZQ_A$ difference spectrum. The prominent feature of trace a in Figure 5 is the intense positive band at 1478 cm^{-1}. Other reproducible features include

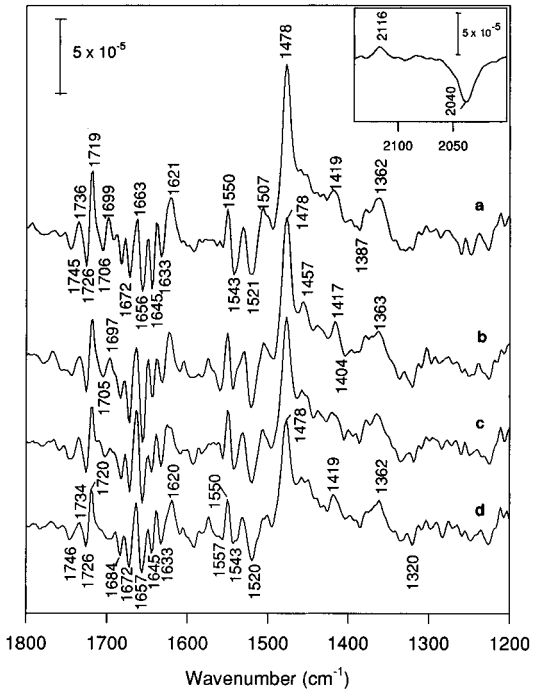

FIGURE 5: Infrared transient spectra of Tris-washed PSII samples in the presence of 10 mM ferro/ferricyanide and 0.1 mM DCMU at pH 6.0. The times after the flash excitation from trace a to trace d are 0−50, 120−170, 240−290, and 360−410 ms, respectively. Three saturating preflashes, spaced 5 s apart, were given to the sample prior to data acquisition. The flash frequency was 0.2 Hz. Each spectrum was averaged over 12 experiments from 3 sample preparations. Inset: characteristic absorptions of ferro/ferricyanide for trace a.

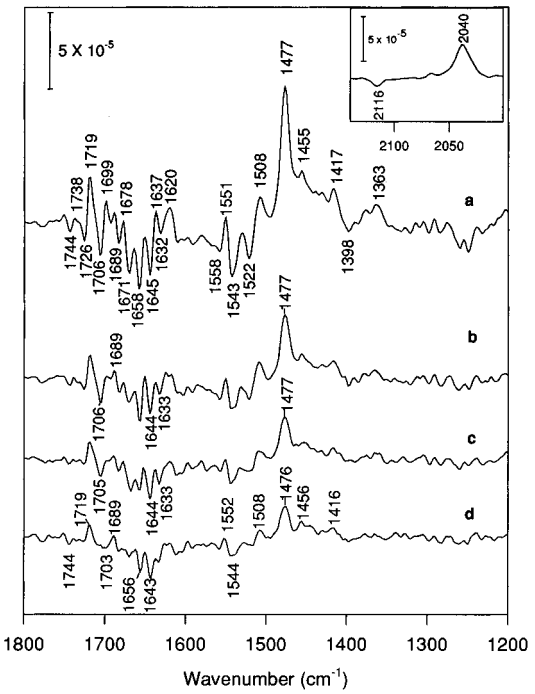

FIGURE 6: Infrared transient spectra of Tris-washed PSII samples in the presence of 10 mM ferro/ferricyanide at pH 6.0. The times after the flash excitation from trace a to trace d are 0−50, 120−170, 240−290, and 360−410 ms, respectively. Three saturating preflashes, spaced 1 s apart, were given to the sample prior to data acquisition. The flash frequency was 1 Hz. Each spectrum was averaged over 18 experiments from 3 sample preparations. Inset: characteristic absorptions of ferro/ferricyanide for trace a.

positive bands at 1736, 1719, 1699, 1663, 1621, 1550, 1507, 1419, and 1362 cm^{-1} and negative bands at 1745, 1726, 1706, 1672, 1656, 1645, 1633, 1543, and 1521 cm^{-1}. The subsequent traces in Figure 5 (traces b−d) show the slow decline in the intensity of the 1478 cm^{-1} band along with the other bands. Within 360 ms after photoexcitation, ~65% Q_A^- but less than 5% Y_Z^{ox} should contribute to trace d according to Figures 2B and 4B. Trace d is identical, except for larger intensity, to the spectrum recorded on longer time scale (720 ms) where ~1% Y_Z^{ox} is left (data not shown). Thus, trace d represents the Q_A^-/Q_A contributions only. Trace d is almost identical to the Q_A^-/Q_A difference spectrum reported earlier (Berthomieu et al., 1992; Hienerwadel et al., 1996; Noguchi et al., 1992). This consistency indicates that less than 5% of Y_Z^{ox} is hardly detectable in the presence of more than 10 times Q_A^- signals.

It is notable that a large differential band at 1706/1699 cm^{-1} is present in traces a and b, but not in trace d (Figure 5) which is attributed to Q_A^-/Q_A only, indicating that this differential band may arise from Y_Z^{ox}/Y_Z. In support of this assignment, the decay of the differential band approximately follows that of Y_Z^{ox} as monitored by EPR (Figure 4B). The 1706/1699 cm^{-1} band is not observed in any spectra recorded after trace d (data not shown).

A comparative FTIR experiment was made under the same conditions except without addition of DCMU. The difference spectra in this case are presented in Figure 6. As shown in the inset, electron transport occurs after excitation as indicated by the characteristic υ(CN) absorptions of ferri/ferrocyanide. In contrast to the DCMU-treated samples, a positive band is observed at 2040 cm^{-1} and a negative band at 2116 cm^{-1}, indicating that the rate of Q_A^- reoxidation by ferricyanide is greater than the rate of reduction of Y_Z^{ox} by ferrocyanide, which is consistent with the fluorescence and EPR measurements (Figures 2A and 4A). The absence of the characteristic non-heme Fe^{2+}/Fe^{3+} positive absorptions at 1338, 1252, and negative absorption at 1228 cm^{-1} (Hienerwadel & Berthomieu, 1995; Noguchi & Inoue, 1995) indicates that Figure 6 contains no contributions from the non-heme iron. Based on the results in Figures 2A and 4A, more than 40% of the Q_A^- and 80% of the Y_Z^{ox} signals contribute to trace a in Figure 6. As shown, an intense band is observed at 1477 cm^{-1}, which corresponds to the 1478 cm^{-1} band in Figure 5. A 1 cm^{-1} shift may not be considered significant since it is within the experimental error of ±1 cm^{-1}. In the absence of DCMU, the intensity of this band drops more rapidly than in the presence of DCMU (Figure 5). Plots of the decay of the 1478 cm^{-1} band in the presence and absence of DCMU are shown in Figure 7. As seen, the decay of the 1478 cm^{-1} band is largely decreased by DCMU. Within 120 ms after the photoexcitation, its intensity drops by more than 50% in the absence of DCMU (open circle), while only by ~14% in the presence of DCMU (solid circle). The sensitivity of the decay of the 1478 cm^{-1} band to DCMU points to its origin from Q_A^-.

In the absence of DCMU, Q_B^-/Q_B may also contribute to the difference spectra (Figure 6). In the bacterial RCs, Q_B^- shows a strong absorption in the region of 1500−1450 cm^{-1}. Recently, we have resolved the $S_2Q_B^-/S_1Q_B$ difference spectrum in PSII (unpublished data). Like the Q_B^- in the bacterial RCs, the Q_B^- of PSII shows an intense absorption at 1480 cm^{-1} which decays slowly. We will discuss the Q_B signal in detail in a forthcoming paper. The absence of

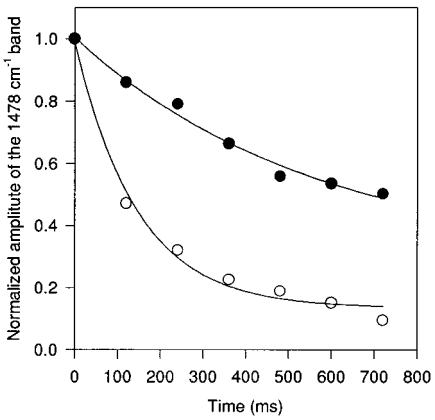

FIGURE 7: Decay kinetics for the 1478 cm^{-1} band in Tris-washed PSII samples in the presence of 10 mM ferro/ferricyanide at pH 6.0. (●) Plus 0.1 mM DCMU; (○) minus DCMU. The signal intensity is normalized under the peak height of trace a (Figures 5 and 6) in both cases. The base line was defined as a flat line from 1900 to 1800 cm^{-1} where there was no IR absorption.

another intense band in the proximity of the 1477 cm^{-1} region and the fast decay of the 1477 cm^{-1} region indicate that any contributions from Q_B to the difference spectra are likely to be very small. However, small contributions from Q_B may become the dominant signals when only residual amounts of Y_Z^{ox} and Q_A^- are left, and this may account for some of the signals on the longer time scales (Figure 7).

With respect to the decay kinetics, some caution should be taken in making a direct comparison of the half-times between the decay of the 1478 cm^{-1} band and the decline in the chlorophyll *a* fluorescence yield. In particular, as described above, the chlorophyll *a* fluorescence (Figure 2) was measured with a pulse-modulated fluorometer. Despite the weak intensity, the monitoring flashes close a fraction of the PSII RCs. As a result, the measured kinetics could be slightly faster than those measured with unmodulated fluorometers (Boerner et al., 1992) which use an excitation condition similar to what we use for the FTIR measurements. Second, the overlapping bands in the region of 1510−1400 cm^{-1} may complicate the determination of the intensity of the 1478 cm^{-1} band, in particular if the overlapping components have different decay kinetics. Finally, the decay of the 1478 cm^{-1} band was measured with a time resolution of 50 ms which is much less than that used in the variable chlorophyll *a* fluorescence measurements (Figure 2). This difference in time resolution may result in an underestimation of the signal amplitude of the 1478 cm^{-1} band, particularly when the signals decay rapidly as in the absence of DCMU. As a consequence, the measured half-times for the 1478 cm^{-1} band will apparently increase. Regardless, however, the overall DCMU effect on the decay of the 1478 cm^{-1} band is obvious (Figure 7).

Interestingly, the differential band at 1706/1699 cm^{-1} is also observed in Figure 6. The relatively large intensity of the differential band is most likely due to the larger ratio of Y_Z^{ox}/Q_A^-. In this case, the decay of the differential band also approximately follows the decay of Y_Z^{ox}. Thus, we conclude that the 1706/1699 cm^{-1} band is associated with Y_Z^{ox}/Y_Z. A similar band at 1704/1697 cm^{-1} was observed previously in the Y_D^{ox}/Y_D difference spectrum and suggested to be from a free carbonyl group or 9-keto carbonyl of a neutral chlorophyll *a* molecule perturbed by Y_D oxidation (Hienerwadel et al., 1996). Although perturbation of certain carbonyl group(s) by Y_Z oxidation may also occur, a more definite assignment requires further detailed investigations. Due to the similar decay kinetics of Y_Z^{ox} and Q_A^- in the absence of DCMU, it is not possible to separate them completely, although traces b, c, and d (Figure 6) show some similarity to what has been reported as the Y_Z^{ox}/Y_Z difference spectrum (Bernard et al., 1995). In future work, we will attempt to resolve the Y_Z^{ox}/Y_Z difference spectrum using the TR-FTIR technique.

CONCLUSION

In conclusion, we have used TR-FTIR spectroscopy to investigate the flash-induced, FTIR difference spectra associated with the redox reactions of Y_Z and Q_A of PSII on the millisecond scale. With this technique, we have been able to obtain the flash-induced $Y_Z^{ox}Q_A^-/Y_ZQ_A$ vibrational difference spectrum as a function of time and to separate out Q_A^-/Q_A signals from Y_Z^{ox}/Y_Z signals by making use of their different decay kinetics in the presence of DCMU. By comparing the $Y_Z^{ox}Q_A^-/Y_ZQ_A$ difference spectrum with the Q_A^-/Q_A difference spectrum, a large differential band at 1706/1699 cm^{-1} has been identified and tentatively associated with Y_Z oxidation. This band may reflect perturbation of local carbonyl group(s) upon Y_Z oxidation. Our results on the decay behavior of the 1478 cm^{-1} band to DCMU confirm that the intense 1478 cm^{-1} band is most likely due to the infrared absorption of the semiquinone anion Q_A^-. In the future, the TR-FTIR method described here can be applied to the study of other time-evolving intermediates in PSII such as the S_i-state transitions.

ACKNOWLEDGMENT

We are grateful to Dr. Marilyn Ball for using her PAM 101 fluorometer and Mr. Denis Herlihy from Bruker Australia for technical help with TR-FTIR measurements. Also we thank Drs. Catherine Berthomieu and Bridgette Barry for valuable comments on the manuscript.

REFERENCES

Babcock, G. T., & Sauer, K. (1975a) *Biochim. Biophys. Acta 376*, 329−344.

Babcock, G. T., & Sauer, K. (1975b) *Biochim. Biophys. Acta 376*, 315−328.

Barry, A. B., & Babcock, G. T. (1987) *Proc. Natl. Acad. Sci. U.S.A. 84*, 7099−7103.

Barry, B. A. (1993) *Photochem. Photobiol. 57*, 179−188.

Bauscher, M., Nabedryk, E., Bagley, K., Breton, J., & Mantele, W. (1990) *FEBS Lett. 261*, 191−195.

Bernard, M. T., MacDonald, G. M., Nguyen, A. P., Debus, R. J., & Barry, B. A. (1995) *J. Biol. Chem. 270*, 1589−1594.

Berthold, D. A., Babcock, G. T., & Yocum, C. F. (1981) *FEBS Lett. 134*, 231−234.

Berthomieu, C., Nabedryk, E., Mäntele, W., & Breton, J. (1990) *FEBS Lett. 269*, 363−367.

Berthomieu, C., Nabedryk, E., Breton, J., & Boussac, A. (1992) in *Research in Photosynthesis* (Murata, N., Ed.) pp 53−56, Kluwer Academic Publishers, Dordrecht, The Netherlands.

Boerner, R. J., Nguyen, A. P., Barry, B. A., & Debus, R. J. (1992) *Biochemistry 31*, 6660−6672.

Bowes, J. M., Crofts, A. R., & Itoh, S. (1979) *Biochim. Biophys. Acta 547*, 320−335.

Debus, R. J. (1992) *Biochim. Biophys. Acta 1102*, 269−352.

Debus, R. J., Barry, B. A., Sithole, I., Babcock, G. T., & McIntosh, L. (1988) *Biochemistry 27*, 9071−9074.

Dekker, J. P., Plijter, J. J., Ouwehand, L., & Van Gorkom, H. J. (1984) *Biochim. Biophys. Acta 767*, 176−179.
Ghanotakis, D. F., Yerkes, C. T., & Babcock, G. T. (1982) *Biochim. Biophys. Acta 682*, 21−31.
Ghanotakis, D. F., Babcock, G. T., & Yerkes, C. T. (1983) *Arch. Biochem. Biophys. 225*, 248−255.
Hienerwadel, R., & Berthomieu, C. (1995) *Biochemistry 34*, 16288−16297.
Hienerwadel, R., Berthomieu, C., Kreutz, W., & Mantele, W. (1992) in *Research in Photosynthesis* (Murata, N., Ed.) pp 49−52, Kluwer Academic Publishers, Dordrecht, The Netherlands.
Hienerwadel, R., Boussac, A., Breton, J., & Berthomieu, C. (1996) *Biochemistry 35*, 15447−15460.
Hoganson, C. W., & Babcock, G. T. (1994) in *Metal Ions in Biological Systems* (Sigel, H., & Sigel, A., Eds.) pp 77−107, Marcel Dekker, Inc., New York.
Ikegami, I., & Katoh, S. (1973) *Plant Cell Physiol. 14*, 829−836.
MacDonald, G. M., Bixby, K. A., & Barry, B. A. (1993) *Proc. Natl. Acad. Sci. U.S.A. 90*, 11024−11028.
MacDonald, G. M., Steenhuis, J. J., & Barry, B. A. (1995) *J. Biol. Chem. 270*, 8420−8428.
Metz, J. G., Nixon, P. J., Rogner, M., Brudvig, G. W., & Diner, B. A. (1989) *Biochemistry 28*, 6960−6969.
Noguchi, T., & Inoue, Y. (1995) *J. Biochem. 118*, 9−12.
Noguchi, T., Ono, T. A., & Inoue, Y. (1992) *Biochemsitry 31*, 5953−5956.
Razeghifard, M. R., Klughammer, C., & Pace, R. J. (1997) *Biochemistry 36*, 86−92.
Ruffle, S., Donnelly, D., Blundell, T. L., & Nugent, J. H. A. (1992) *Photosynth. Res. 34*, 287−300.
Schelvis, J. P. M., van Noort, P. I., Anartsma, T. J., & van Gorkom, H. J. (1994) *Biochim. Biophys. Acta 1184*, 242−250.
Thibodeau, D. L., Nabedryk, E., Hienerwadel, R., Lenz, F., Mäntele, W., & Breton, J. (1990) *Biochim. Biophys. Acta 1020*, 253−259.
Vermaas, W. F. J., Rutherford, A. W., & Hansson, Ö. (1988) *Proc. Natl. Acad. Sci. U.S.A. 85*, 8477−8481.
Yerkes, C. T., & Babcock, G. T. (1980) *Biochim. Biophys. Acta 590*, 360−372.

BI970815T